(12)

HDL-TR-2090
July 1986

Electric and Magnetic Field Coupling Through a Braided-Shield Cable: Transfer Admittance and Transfer Impedance

by Huey A. Roberts
Susan B. MacDonald
Joseph Capobianco

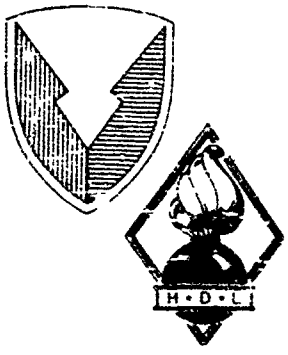

U.S. Army Laboratory Command
Harry Diamond Laboratories
Adelphi, MD 20783-1197

The findings in this report are not to be construed as an official Department of the Army position unless so designated by other authorized documents.

Citation of manufacturers' or trade names does not constitute an official indorsement or approval of the use thereof.

Destroy this report when it is no longer needed. Do not return it to the originator

UNCLASSIFIED

SECURITY CLASSIFICATION OF THIS PAGE *(When Data Entered)*

ADA 171 490

REPORT DOCUMENTATION PAGE

READ INSTRUCTIONS BEFORE COMPLETING FORM

1. REPORT NUMBER: HDL-TR-2090	2. GOVT ACCESSION NO.
3. RECIPIENT'S CATALOG NUMBER	
4. TITLE *(and Subtitle)*: Electric and Magnetic Field Coupling Through a Braided-Shield Cable, Transfer Admittance and Transfer Impedance	5. TYPE OF REPORT & PERIOD COVERED: Technical Report
6. PERFORMING ORG. REPORT NUMBER	
7. AUTHOR(s): Huey A. Roberts, Susan B. MacDonald, Joseph Capobianco	8. CONTRACT OR GRANT NUMBER(s)
9. PERFORMING ORGANIZATION NAME AND ADDRESS: Harry Diamond Laboratories, 2800 Powder Mill Road, Adelphi, MD 20783-1197	10. PROGRAM ELEMENT, PROJECT, TASK AREA & WORK UNIT NUMBERS: HDL Project: E9B3E0
11. CONTROLLING OFFICE NAME AND ADDRESS: U.S. Army Laboratory Command, 2800 Powder Mill Road, Adelphi, MD 20783-1145	12. REPORT DATE: July 1986
	13. NUMBER OF PAGES: 22
14. MONITORING AGENCY NAME & ADDRESS *(if different from Controlling Office)*	15. SECURITY CLASS. *(of this report)*: UNCLASSIFIED
	15a. DECLASSIFICATION/DOWNGRADING SCHEDULE

16. DISTRIBUTION STATEMENT *(of this Report)*

Approved for public release; distribution unlimited.

17. DISTRIBUTION STATEMENT *(of the abstract entered in Block 20, if different from Report)*

18. SUPPLEMENTARY NOTES

19. KEY WORDS *(Continue on reverse side if necessary and identify by block number)*

Shielded cable
Cable coupling
Transfer impedance
Transfer admittance

20. ABSTRACT *(Continue on reverse side if necessary and identify by block number)*

Electric and magnetic coupling parameters are measured for a braided-shield cable. Starting with a general solution for the internal response of an externally excited cable, simple expressions which relate the coupling parameters to the internal and external currents and voltages result when the electrically short line approximation is used. These expressions are applied to experimental configurations in which the external excitation is either predominately magnetic or electric, and the internal loading is configured to exclude either the electrically or magnetically induced internal currents. The experimental results are compared with theoretical calculations appearing in the literature, and the relative importance of the electric and magnetic coupling effects is discussed.

DD FORM 1 JAN 73 1473 EDITION OF 1 NOV 65 IS OBSOLETE

UNCLASSIFIED

SECURITY CLASSIFICATION OF THIS PAGE *(When Data Entered)*

CONTENTS

FIGURES

1. INTRODUCTION

The response of a braided-shield cable to external electromagnetic excitation in the presence of a third parallel conductor (e.g., the earth) can be obtained by considering a set of two coupled transmission lines. The external line is formed by the third conductor and the outer surface of the cable shield, and the internal line is just the coaxial cable itself. Theoretical analyses of this problem are found elsewhere in the literature.[1-5] Coupling to the internal line (i.e., penetration of the magnetic and electric fields) results from both the finite conductivity of the shield and the presence of apertures in the weaving of the braided wire.

The electric and magnetic fields associated with the external transmission line are relatively unperturbed by the imperfections of a typical cable shield. That is, the reaction of the internal line on the external region is negligible. Because of the weak coupling between the two transmission lines, a good approximate solution for the response of the internal line can be obtained in a two-step process using simple two-conductor transmission-line equations. The first step is to determine the tangential magnetic and normal electric fields at the outer surface of the cable shield for the particular external excitation, assuming the shield to be a solid cylindrical conductor. Then, assuming that the coupling parameters between these surface fields and the interior are known, one can compute the currents and voltages along the internal transmission line.

Measurements which directly determine the magnitude of the electric field coupling have apparently not been published, even though theoretical analyses suggest that the electric and magnetic coupling effects are comparable for many cables.[1,5] The published results are measurements of the magnetic field coupling alone or a mixture of the electric and magnetic field coupling effects. Frankel[4] has reviewed and commented on a number of results published before 1971 and points out that the effects of these two types of coupling depend not only on the relative magnitudes of the coupling parameters but also on the length of the cable, the terminations of both the internal and external transmission lines, and the orientation and polarization of the externally impressed fields. A more recent approach by Martin and Emert[6] uses a curve-fitting routine to estimate both the electric and magnetic field coupling parameters.

---

[1] E. F. Vance, Comparison of Electric and Magnetic Coupling Through Braided Wire Shields, Stanford Research Institute, Technical Report No. AFWL-TR-73-7 (1973).

[2] E. V. Vance and H. Chang, Shielding Effectiveness of Braided Wire Shields, Air Force Weapons Laboratory, Technical Memorandum No. 16, AFWL Contract F29601-69-C-0127 (November 1971).

[3] K. S. H. Lee and C. E. Baum, Application of Modal Analysis to Braided-Shield Cables, IEEE Trans. Electromagn. Compat., EMC-17, No. 3 (August 1975).

[4] S. Frankel, Terminal Response of Braided-Shield Cables to External Monochromatic Electromagnetic Fields, IEEE Trans. Electromagn. Compat., EMC-16, No. 1 (February 1974).

[5] E. F. Vance, Coupling to Shielded Cables, Wiley-Interscience, New York (1978), pp 148-149.

[6] A. R. Martin and S. E. Emert, The Shielding Effectiveness of Long Cables, II: L_T and GTR, IEEE Trans. Electromagn. Compat., EMC-22, No. 4 (November 1980).

For a cable shield having a high degree of optical coverage (e.g., a double shield) the relative effects due to electric field coupling should be small. Merewether and Ezell[7] investigated the response of an RG-214 coaxial cable. They measured the magnetic field coupling and determined an upper bound for the electric field coupling parameter. Their results show that for an RG-214 cable the electric field coupling is relatively insignificant.

In this paper we present experimental results which determine the magnitudes of both the electric and magnetic coupling coefficients for an RG-8 coaxial cable. This particular cable was chosen because of the relatively large apertures in the braided shield.

2. GENERAL CONSIDERATIONS

The transfer of electromagnetic energy to the interior of a shielded cable occurs both by diffusion and by penetration through apertures in the braided structure. The diffusion is proportional to the magnetic field only, because of the relatively high conductivity of the metal. Both the magnetic and electric fields couple through the apertures, however, and theory predicts the resulting effects to be comparable.[1,5]

The problem of fields coupling through apertures is discussed by Vance and Chang.[2] They show that the magnetic field penetration to the cable interior can be expressed as a series inductive coupling proportional to the frequency and to the tangential magnetic field at the outer surface of the shield. Likewise, the penetration of the electric field can be expressed as a shunt capacitive coupling proportional to the frequency and to the normal electric field at the outer surface of the shield. The tangential magnetic field at the surface is proportional to the shield current, and the normal electric field at the surface is proportional to the product of the capacitance per unit length and the transverse voltage of the external transmission line. Hence, for any given frequency, the coupling can be represented as equivalent series and shunt sources, proportional respectively to the current and transverse voltage (assuming uniform capacitance) of the external transmission line. Since the cables are of uniform construction with aperture spacing small compared to the wavelengths of interest, the sources can be treated as being continuously distributed along the length of the cable.

In this discussion we assume that the fields are symmetric about the cable axis. For the laboratory arrangement used here this is true since the inter-

---

[1] E. F. Vance, Comparison of Electric and Magnetic Coupling Through Braided Wire Shields, Stanford Research Institute, Technical Report No. AFWL-TR-73-7 (1973).

[2] E. V. Vance and H. Chang, Shielding Effectiveness of Braided Wire Shields, Air Force Weapons Laboratory, Technical Memorandum No. 16, AFWL Contract F29601-69-C-0127 (November 1971).

[5] E. F. Vance, Coupling to Shielded Cables, Wiley-Interscience, New York (1978), pp 148-149.

[7] D. E. Merewether and T. F. Ezell, The Effect of Mutual Inductance and Mutual Capacitance of the Transient Response of Braided-Shield Coaxial Cables, IEEE Trans. Electromagn. Compat., EMC-18, No. 1 (February 1976).

nal and external lines are coaxial. In most practical situations this is not true, but one can consider average values about the outer periphery of the shield.[4]

3. SOURCE COUPLING PARAMETERS

The per-unit-length coupling parameters referred to as the transfer impedance, Z_T, for the series source, and transfer admittance, Y_T, for the shunt source, are expressed as[5]

$$Z_T = M_d + j\omega M_{12} \tag{1}$$

and

$$Y_T = j\omega C_{12} \quad . \tag{2}$$

The first term of the transfer impedance relation is the diffusion parameter and can be expressed as

$$M_d = \frac{R_0(1 + j)T/\delta}{\sinh[(1 + j)T/\delta]} \quad , \tag{3}$$

where R_0 is the dc resistance per unit length of the shield, T is the effective thickness of the shield, $\delta = (2/\omega\mu\sigma)^{1/2}$ is the skin depth in the shield, ω is the angular frequency, and σ and μ are respectively the electrical conductivity and the magnetic permeability of the shield material. The constants M_{12} and C_{12}, the magnetic and electric field coupling coefficients for apertures, are determined experimentally, although approximate expressions have been derived theoretically.[1,5] The diffusion term decreases rapidly with frequency, and hence the high-frequency coupling is dominated by aperture effects and increases linearly with frequency.

Lee and Baum[3] show that in general Z_T and Y_T appear not only in the source terms but are also combined with the distributed transmission-line coefficients. For most coaxial cables, however, M_{12} and C_{12} are small compared to the corresponding inductance and capacitance of the cable and need appear only in the source terms of the differential equations which describe the coupling.

4. INTERNAL RESPONSE

In this section we determine the currents flowing in the center conductor of a coaxial cable resulting from the penetration of external electromagnetic

---

[1] E. F. Vance, Comparison of Electric and Magnetic Coupling Through Braided Wire Shields, Stanford Research Institute, Technical Report No. AFWL-TR-73-7 (1973).

[3] K. S. H. Lee and C. E. Baum, Application of Modal Analysis to Braided-Shield Cables, IEEE Trans. Electromagn. Compat., EMC-17, No. 3 (August 1975).

[4] S. Frankel, Terminal Response of Braided-Shield Cables to External Monochromatic Electromagnetic Fields, IEEE Trans. Electromagn. Compat., EMC-16, No. 1 (February 1974).

[5] E. F. Vance, Coupling to Shielded Cables, Wiley-Interscience, New York (1978), pp 148-149.

fields through the cable shield. The shield is driven at one end with respect to a third conductor to which the shield is characteristically terminated at the opposite end. Then, for an electrically short cable we investigate the interior terminal currents for different terminating impedances and show that one can selectively measure the currents induced by the magnetic or electric fields. We then terminate the external line in ways which substantially reduce either the external magnetic or electric fields.

Consider a shielded coaxial cable of length ℓ with exterior current and voltage given by $I_s(\omega,\xi) = I_0(\omega)e^{-\gamma_0\xi}$ and $V_0(\omega,\xi) = Z_{0e}I_s(\omega,\xi)$, where Z_{0e} is the characteristic impedance of the external line, ξ is the distance from the driven end, and $\gamma_0 = j\omega/c$. We can obtain the center conductor current at the coordinate y by integrating the magnetic and electric field sources with the corresponding point-source response functions. Thus, the magnetic and electric currents in the center conductor are

$$I_m(\omega,y) = Z_T(\omega)I_0(\omega)\int_0^{\ell} e^{-\gamma_0\xi} H_m(\omega,y,\xi)\, d\xi \tag{4}$$

and

$$I_e(\omega,y) = -Y_T(\omega)Z_{0e}I_0(\omega)\int_0^{\ell} e^{-\gamma_0\xi} H_e(\omega,y,\xi)\, d\xi \quad . \tag{5}$$

The functions $H_m(\omega,y,\xi)$ and $H_e(\omega,y,\xi)$ are the currents at y due respectively to a series voltage source and shunt current source at ξ, both of unit amplitude with harmonic time dependence $e^{j\omega t}$. The time-dependent term is suppressed in this discussion.

A derivation of the point-source response function is given by Schelkunoff[8] (chapter 7). The results, expressed differently, are

$$H_m = \frac{1}{2Z_0D(\ell)}\left[e^{-\gamma|y-\xi|} + R_2e^{-2\gamma\ell}e^{\gamma(y+\xi)} + R_1e^{-\gamma(y+\xi)} + R_1R_2e^{-2\gamma\ell}e^{\gamma|y-\xi|}\right] \tag{6}$$

and

$$H_e = \frac{1}{2D(\ell)}\left[\pm e^{-\gamma|y-\xi|} + R_2e^{-2\gamma\ell}e^{\gamma(y+\xi)} - R_1e^{-\gamma(y+\xi)} \mp R_1R_2e^{-2\gamma\ell}e^{\gamma|y-\xi|}\right], \tag{7}$$

[8] S. A. Schelkunoff, Electromagnetic Waves, D. Van Nostrand Co., New York (1943).

where the upper signs in equation (7) correspond to $y > \xi$ and the lower signs to $y < \xi$. Z_0 is the characteristic impedance of the internal line,

$$R_1 = \frac{Z_0 - Z_1}{Z_0 + Z_1} \quad , \quad R_2 = \frac{Z_0 - Z_2}{Z_0 + Z_2} \quad , \quad \gamma = \alpha + j\,\frac{\omega}{v} \quad ,$$

and $D(\ell) = 1 - R_1 R_2 e^{-2\gamma\ell}$, where α and v are respectively the attenuation constant and the propagation velocity associated with the internal line. The impedances Z_1 and Z_2 terminate the internal line at $y = 0$ (the driven end) and $y = \ell$, respectively.

With $\Gamma_1 = \gamma - \gamma_0$, $\Gamma_2 = \gamma + \gamma_0$,

$$P(y) = \int_0^y e^{\Gamma_1 \xi}\, d\xi \quad ,$$

and

$$Q(y) = \int_y^{\ell} e^{-\Gamma_2 \xi}\, d\xi \quad ,$$

equations (4) and (5) become

$$I_m(y,\omega) = \frac{Z_T(\omega) I_0(\omega)}{2Z_0} \left[e^{\gamma y} \left(Q(y) + \frac{R_2 e^{-2\gamma\ell} \left(P(\ell) + R_1 Q(0) \right)}{D(\ell)} \right) \right.$$

$$\left. + e^{-\gamma y} \left(P(y) + \frac{R_1 \left(N(\ell) + R_2 e^{-2\gamma\ell} P(\ell) \right)}{D(\ell)} \right) \right] \tag{8}$$

and

$$I_e(y,\omega) = \frac{-Y_T(\omega) Z_{0e} I_0(\omega)}{2} \left[e^{\gamma y} \left(-Q(y) + \frac{R_2 e^{-2\gamma\ell} \left(P(\ell) - R_1 Q(0) \right)}{D(\ell)} \right) \right.$$

$$\left. + e^{-\gamma y} \left(P(y) - \frac{R_1 \left(N(\ell) - R_2 e^{-2\gamma\ell} P(\ell) \right)}{D(\ell)} \right) \right] . \tag{9}$$

We now examine the terminal responses for three different termination configurations.

Case I. Both ends of internal line terminated characteristically: $Z_1 = Z_2 = Z_0$.

From equations (8) and (9) at y = 0, we find that

$$I_m(0) = \frac{Z_T(\omega)I_0(\omega)}{2Z_0\Gamma_2}\left[1 - e^{-\Gamma_2 \ell}\right] \tag{10}$$

and

$$I_e(0) = \frac{Y_T(\omega)Z_{0e}I_0(\omega)}{2\Gamma_2}\left[1 - e^{-\Gamma_2 \ell}\right] \quad , \tag{11}$$

and at $y = \ell$

$$I_m(\ell) = \frac{Z_T(\omega)I_0(\omega)}{2Z_0\Gamma_1}\left[e^{-\gamma_0 \ell} - e^{-\gamma \ell}\right] \tag{12}$$

and

$$I_e(\ell) = \frac{-Y_T(\omega)Z_{0e}I_0(\omega)}{2\Gamma_1}\left[e^{-\gamma_0 \ell} - e^{-\gamma \ell}\right] \quad . \tag{13}$$

If only first-order terms for an electrically short line are retained, the bracketed terms in equations (10) to (13) become ℓ. Then

$$I(0) = I_m(0) + I_e(0) = \frac{Z_T(\omega)I_0(\omega)\ell}{2Z_0}\left[1 + \frac{Y_T(\omega)Z_{0e}Z_0}{Z_T(\omega)}\right] \tag{14}$$

and

$$I(\ell) = I_m(\ell) + I_e(\ell) = \frac{Z_T(\omega)I_0(\omega)\ell}{2Z_0}\left[1 - \frac{Y_T(\omega)Z_{0e}Z_0}{Z_T(\omega)}\right] \quad . \tag{15}$$

By measuring the current at both ends (or equivalently measuring at one end and driving at both ends), one obtains from (14) and (15)

$$Z_T = Z_0 \frac{I(0) + I(\ell)}{I_0\ell} \tag{16}$$

and

$$Y_T = \frac{I(0) - I(\ell)}{Z_{0e}I_0\ell} \quad . \tag{17}$$

At high frequencies where aperture coupling dominates, only the magnitudes of $I(0)$ and $I(\ell)$ are required to obtain M_{12} and C_{12}.

Case II. Driven end of internal line characteristically terminated, far end shorted: $Z_1 = Z_0$, $Z_2 = 0$.

Equations (8) and (9) now yield at y = 0

$$I_m(0) = \frac{Z_T I_0(\omega)}{2Z_0}\left[Q(0) + e^{-2\gamma\ell}P(\ell)\right] \tag{18}$$

and

$$I_e(0) = -Y_T Z_{0e} I_0(\omega)\left[-Q(0) + e^{-2\gamma\ell}P(\ell)\right] \quad . \tag{19}$$

Retaining only first-order terms, we obtain

$$I_m(0) = \frac{Z_T I_0(\omega)\ell}{Z_0} \tag{20}$$

and

$$I_e(0) = 0 \quad .$$

Case III. Driven end characteristically terminated, far end open: $Z_1 = Z_0$, $Z_2 = \infty$.

Again, from equations (8) and (9), at y = 0 we get

$$I_m = \frac{Z_T I_0(\omega)}{2Z_0}\left[Q(0) - e^{-2\gamma\ell}P(\ell)\right] \approx 0$$

and

$$\begin{aligned} I_e &= \frac{-Y_T Z_{0e} I_0(\omega)}{2}\left[-Q(0) - e^{-2\gamma\ell}P(\ell)\right] \\ &\approx Y_T Z_{0e} I_0(\omega)\ell \quad . \end{aligned} \tag{21}$$

Thus, for an electrically short line, current contributions induced by the electric and magnetic fields can be selectively excluded by respectively short circuiting and open circuiting the far-end termination.

In addition, the external electric or magnetic field can be substantially reduced for the electrically short line by changing the external drive circuit. If the external line is terminated in $Z_\ell = 0$, then, for a sufficiently short line, the normal electric field will be negligible. On the other hand, if $Z_\ell = \infty$, then it is possible to establish a normal electric field with negligible magnetic field.

It would be prudent in attempting to measure the coupling parameters to adjust both the internal and external circuit for optimum conditions. When an electrically short line is used, Z_T would be measured with $Z_\ell = Z_2 = 0$ and $Z_1 = Z_0$. Likewise, to measure Y_T the terminations would be $Z_1 = Z_0$ and $Z_\ell = Z_2 = \infty$. Then from equations (20) and (21),

$$Z_T(\omega) = \frac{Z_0 I_m(\omega)}{I_s(\omega)\ell} \tag{22}$$

and

$$Y_T(\omega) = \frac{I_e(\omega)}{V_0(\omega)\ell} \quad , \tag{23}$$

where $I_s(\omega)$ is the external shield current and $V_0(\omega)$ the transverse voltage for the two external line configurations.

The transfer impedance and transfer admittance are usually defined[5] in terms of the internal open-circuit voltage and short-circuit current, respectively. However, for a typical cable, both Z_T and Y_T are quite small and, hence, to a very good approximation $Z_0 I_m$ and I_e in equations (22) and (23) are respectively equal to the open-circuit voltage and short-circuit current.

5. LABORATORY MEASUREMENTS

A 20-cm-long sample of RG-8 coaxial cable shield was positioned coaxially inside a 50-cm-long cylindrical aluminum tube having a 10-cm inside diameter. The additional length of the external circuit, which included copper-tube extensions from the braided shield, was intended to minimize end effects in the sample region. We constructed the test sample by soldering a copper tube around all but 20 cm of a 48-cm length of cable, the internal line. A shorting screw, accessible through the tubular extension opposite the measurement end, was used to open circuit and short circuit the internal line and thus exclude the magnetic and electric contributions, respectively, to the internal currents. The insulating jacket remained around the braided shield in order to maintain the natural contact resistance of the braided weave.

Figure 1 shows the experimental configurations. The external circuits were driven with a capacitive discharge pulser fired through a self-breaking spark gap. The resulting shield current I_s in figure 1(a) and the resistor current I_r in figure 1(b) had rise times of approximately 15 ns, e-fold decay times of 3 μs, and peak amplitudes of approximately 80 A. Both I_s and I_r were measured using a Singer 91550-3 current probe. A Tektronix CT-1 probe was used for the internal measurements. The spectral content of the external and internal current pulses was recorded on Polaroid film using an HP 141T spectrum analyzer and camera located inside the shielded enclosure. The pulser operated at approximately one pulse per second as the analyzer slowly swept through the range of frequency, sampling each pulse.

[5] E. F. Vance, Coupling to Shielded Cables, Wiley-Interscience, New York (1978), pp 148-149.

The experimental results for the magnitudes of Z_T and Y_T using equations (22) and (23) are shown as dots in figure 2. The straight line through the Y_T data has a slope of 1 and yields an electric field coupling constant $C_{12} = Y_T/\omega$ of 2.25×10^{-14} F/m. As shown below, the departure from the straight line at higher frequencies can be attributed to the presence of unwanted magnetic field contributions to the internal currents.

The line through the high-frequency region of the Z_T data has a slope of 0.9, deviating from the theoretical value of 1. The low-frequency Z_T data correspond to a dc resistance of 7.9×10^{-3} Ω/m. The measured resistance of a 10-m length of identical cable using a precision milliohm meter was 74 mΩ.

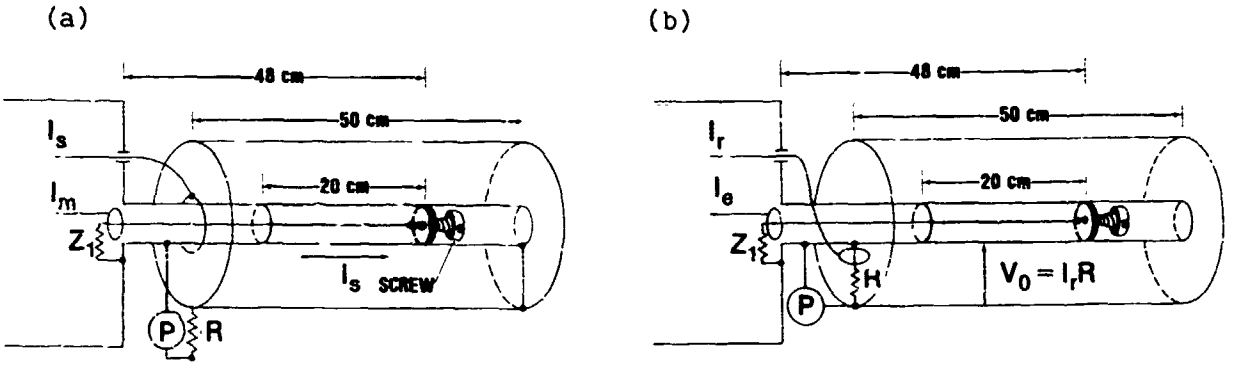

Figure 1. Experimental configuration for measuring (a) transfer impedance and (b) transfer admittance.

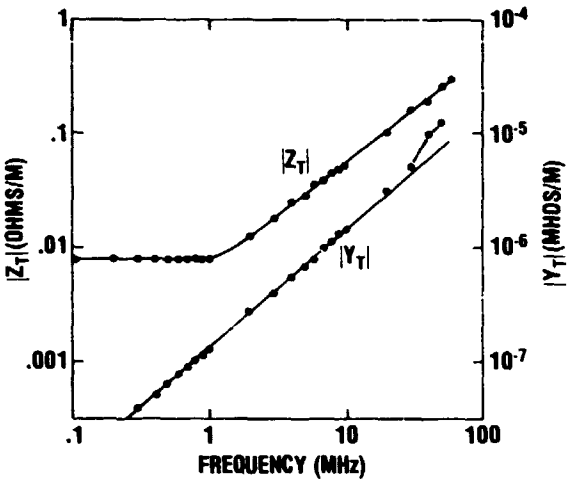

Figure 2. Transfer impedance and transfer admittance of an RG-8 coaxial cable.

Measurements were made to investigate the presence of both electric and magnetic field coupling to the internal circuit with the external circuit configured to produce either the electric or magnetic field. For the external circuit configuration in figure 1(a), the ratio I_{oc}/I_{sc} of the internal currents through the 50-Ω termination was recorded for the shorting screw open circuited and short circuited. Likewise, for the external configuration of figure 1(b), the ratio I_{sc}/I_{oc} was recorded. These data, shown in figure 3, demonstrate the significance of the internal circuit configuration for measuring the coupling parameters. For example, at 30 MHz the error in Y_T using the configuration in figure 1(b) is almost negligible. However, from figure 3 it is clear that a very significant error would result if the internal circuit were terminated in 50 Ω at both ends.

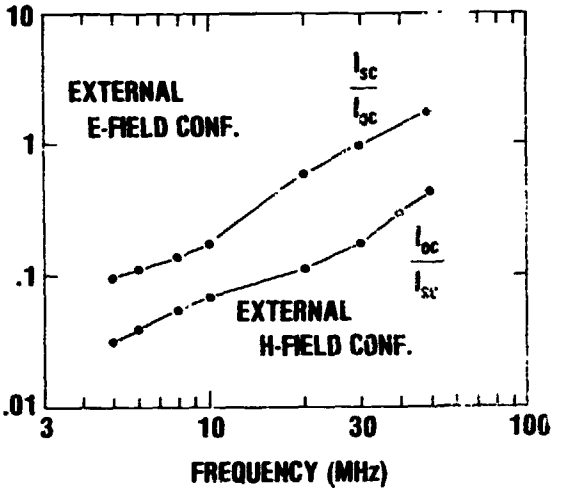

Figure 3. Ratios of coupling through shield: (upper curve) magnetic to electric field, external circuit configured to produce electric field; (lower curve) electric to magnetic field, external circuit configured to produce magnetic field.

The electric field coupling measurements could be improved at higher frequencies if the internal load resistance Z_1 were increased. Thus, the magnetic field contributions would be reduced, whereas the electric field contributions would be unchanged so long as $Z_1 << 1/Y_T\ell$. Similarly, the smallest value of Z_1 such that $Z_1 >> Z_T\ell$ would yield the best results when electric field coupling contributes to the internal currents. The load resistance Z_1 must also be significantly larger than the insertion impedance of the probe used to measure the internal current. A Tektronix CT-1 probe for example has an insertion impedance of approximately 1 Ω.

6. DISCUSSION

A problem encountered in describing the electric field coupling in terms of a transfer admittance is that the proportionality between the normal electric field and the transverse voltage of the external circuit includes the capacitance of the external circuit. Hence, a transfer admittance measurement in the laboratory is dependent on the geometry and dielectric material of the experimental configuration. For this reason it is convenient to define a transfer ratio as the measured transfer admittance divided by the capacitance per unit length C_d of the external drive circuit used in the measurement. The transfer ratio is then multiplied by the corresponding capacitance for any configuration in which the admittance is used to compute the electric field coupling. A similar problem does not exist with the transfer impedance, since the proportionality between the tangential magnetic field and the shield current depends only on the shield diameter.

When the external transverse voltage and shield current are related by $V_0 = Z_{0e}I_s$, the ratio of the magnetic to electric field coupling to the internal line is given by

$$R_{m,e} = \frac{Z_T}{Y_T Z_{0e} Z_0} \quad . \tag{24}$$

In our laboratory experiments $Z_{0e} = 138\ \Omega$ and $Z_0 = 50\ \Omega$. Then from the measured data at 5 and 10 MHz we obtain $R_{m,e} = 5.9$ and 5.3, respectively. The same ratio would be observed for other drive geometries which have the same dielectric medium, air in this case. For example, we could have used the transfer ratio Y_T/C_d and multiplied by the capacitance of the drive circuits. Then

$$\frac{Z_T}{(Y_T/C_d)C_d Z_{0e} Z_0} = \frac{Z_T(\mu\varepsilon)^{-1/2}}{(Y_T/C_d)Z_0} \quad , \tag{25}$$

where μ and ε are respectively the magnetic permeability and dielectric permittivity of the external drive circuit.

Equation (24) has been computed by Vance[5] for air dielectric inside and outside the shield as a function of the braid weave-angle. For a weave-angle of 30 degrees corresponding to an RG-8 shield, the computed ratio is approximately 1.5. In order to compare our measured results with the computed ratio, a correction is required to account for the dielectric insulation of the RG-8 cable. The correction pertains only to the electric field coupling term, Y_T. If the effect of the thin protective outer jacket is negligible, then the correction factor[9] to be applied to the computed value is

$$\frac{2\varepsilon_r}{1 + \varepsilon_r} = 1.4 \quad ,$$

where $\varepsilon_r = 2.4$ is the relative dielectric constant of the polyethylene insulation. Thus the computed ratio for an RG-8 cable becomes $1.5/1.4 \approx 1$ as compared to the measured values of between 5 and 6.

The discrepancy between the measured and computed ratios may result from an overly simplified model of a braided-shield cable used in the calculations. The model does not account for the finite thickness of the shield or the interwoven structure and associated contact resistances. Madel[10] explains another magnetic field coupling mechanism, termed "porpoising," which results

---

[5] E. F. Vance, Coupling to Shielded Cables, Wiley-Interscience, New York (1978), pp 148-149.

[9] L. Marin, Effects of a Dielectric Jacket of a Braided-Shield Cable on EMP Coupling Calculations, Interaction Notes, Note 178, Air Force Weapons Laboratory, Kirtland Air Force Base, NM (May 1974).

[10] P. J. Madel, Contact Resistance and Porpoising Effects in Braid Shielded Cables, IEEE International Symposium on Electromagnetic Compatibility (1980), pp 206-210.

from the braided weave pattern and adds to the transfer impedance. The porpoising mechanism can be dominant in some shields. Moreover, the thin-wall approximation tends to exaggerate the electric field coupling. For a shield of finite thickness, some of the field lines would bend and terminate on the shield rather than on the center conductor, thus reducing the effective area of the aperture.

From figure 3 it is clear that for our 0.5-m external line it would not be possible to accurately measure the electric field coupling above several megahertz without open circuiting the internal line as shown in figure 1(b). An earlier version of this experiment,[11] using a 20-cm sample length without the cylindrical extensions shown in figure 1, yielded essentially the same results. Therefore, the lengths of both the external and internal lines could have been smaller in the experiments reported here. In the earlier measurements using the shorter line, the departure from the straight line in the Y_T data at 40 and 50 MHz was not observed.

7. CONCLUSIONS

Our experimental results show that for a braided-shield cable, the electric field contribution to the internal cable responses is relatively unimportant at low frequencies where the diffusion component of the magnetic field coupling is dominant. At higher frequencies, however, the electric field coupling can be significant and, depending on the configuration and external excitation of the cable, should be included in estimating interference effects. Our measurements indicate that, for the RG-8 coaxial cable evaluated, the electric field coupling is less important relative to the magnetic field coupling than had been expected.

[11] S. B. MacDonald, Electric and Magnetic Coupling Measurements of Braided-Shield Cables, 23rd Annual Student Technical Symposium, Harry Diamond Laboratories (September 1982), pp 149-157.

LITERATURE CITED

1. E. F. Vance, Comparison of Electric and Magnetic Coupling Through Braided Wire Shields, Stanford Research Institute, Technical Report No. AFWL-TR-73-7 (1973).

2. E. V. Vance and H. Chang, Shielding Effectiveness of Braided Wire Shields, Air Force Weapons Laboratory, Technical Memorandum No. 16, AFWL Contract F29601-69-C-0127 (November 1971).

3. K. S. H. Lee and C. E. Baum, Application of Modal Analysis to Braided-Shield Cables, IEEE Trans. Electromagn. Compat., EMC-17, No. 3 (August 1975).

4. S. Frankel, Terminal Response of Braided-Shield Cables to External Monochromatic Electromagnetic Fields, IEEE Trans. Electromagn. Compat., EMC-16, No. 1 (February 1974).

5. E. F. Vance, Coupling to Shielded Cables, Wiley-Interscience, New York (1978), pp 148-149.

6. A. R. Martin and S. E. Emert, The Shielding Effectiveness of Long Cables, II: L_T and GTR, IEEE Trans. Electromagn. Compat., EMC-22, No. 4 (November 1980).

7. D. E. Merewether and T. F. Ezell, The Effect of Mutual Inductance and Mutual Capacitance of the Transient Response of Braided-Shield Coaxial Cables, IEEE Trans. Electromagn. Compat., EMC-18, No. 1 (February 1976).

8. S. A. Schelkunoff, Electromagnetic Waves, D. Van Nostrand Co., New York (1943).

9. L. Marin, Effects of a Dielectric Jacket of a Braided-Shield Cable on EMP Coupling Calculations, Interaction Notes, Note 178, Air Force Weapons Laboratory, Kirtland Air Force Base, NM (May 1974).

10. P. J. Madel, Contact Resistance and Porpoising Effects in Braid Shielded Cables, IEEE International Symposium on Electromagnetic Compatibility (1980), pp 206-210.

11. S. B. MacDonald, Electric and Magnetic Coupling Measurements of Braided-Shield Cables, 23rd Annual Student Technical Symposium, Harry Diamond Laboratories (September 1982), pp 149-157.

DISTRIBUTION

ADMINISTRATOR
DEFENSE TECHNICAL INFORMATION CENTER
CAMERON STATION, BUILDING 5
ATTN DTIC-DDA (12 COPIES)
ALEXANDRIA, VA 22304-6145

ASSISTANT TO THE SECRETARY OF DEFENSE
ATOMIC ENERGY
ATTN EXECUTIVE ASSISTANT
WASHINGTON, DC 20301

DIRECTOR
DEFENSE COMMUNICATIONS AGENCY
ATTN CODE B410
ATTN CODE B430
WASHINGTON, DC 20305

DIRECTOR
COMMAND CONTROL ENGINEERING CENTER
ATTN C-661, DR. T. TRINKLE
ATTN C-630, R. LIPP
WASHINGTON, DC 20305

DIRECTOR
DEFENSE COMMUNICATIONS ENGINEERING CENTER
ATTN CODE R400
ATTN CODE R123, TECH LIB
ATTN CODE R111, SICA
1860 WIEHLE AVENUE
RESTON, VA 22090

ASSISTANT CHIEF OF STAFF FOR
INFORMATION MANAGEMENT
COMMAND SYSTEMS INTEGRATION OFFICE
ATTN DAMO-C4Z, COL D. GRIGGS
THE PENTAGON
WASHINGTON, DC 20301

DIRECTOR
DEFENSE INTELLIGENCE AGENCY
ATTN DB-4C2, D. SPOHN
WASHINGTON, DC 20301

CHAIRMAN
JOINT CHIEFS OF STAFF
ATTN J-3
ATTN C3S
WASHINGTON, DC 20301

NATIONAL COMMUNICATIONS SYSTEM
DEPARTMENT OF DEFENSE
OFFICE OF THE MANAGER
ATTN NCS-TS, D. BODSON
WASHINGTON, DC 20305

DIRECTOR
DEFENSE NUCLEAR AGENCY
ATTN NATA
ATTN RAEV

DEFENSE NUCLEAR AGENCY (Cont'd)
ATTN DDST
ATTN RAEE
ATTN TITL
WASHINGTON, DC 20305

OFFICE OF UNDERSECRETARY OF DEFENSE
RESEARCH & ENGINEERING
ATTN DMSSO
2 SKYLINE PLACE
SUITE 1403
5203 LEESBURG PIKE
FALLS CHURCH, VA 22041

UNDER SECY OF DEF FOR RSCH & ENGRG
DEPARTMENT OF DEFENSE
ATTN STRATEGIC & SPACE SYS 9OSO RM 3E129
ATTN STRAT & THEATER NUC FORCES
WASHINGTON, DC 20301

DEPUTY DIRECTOR FOR THEATRE/TACTICAL C3
SYSTEMS
JOINT STAFF
WASHINGTON, DC 20301

COMMANDER-IN-CHIEF
US FORCES, EUROPE
ATTN ECC3S
APO, NY 09128

ASSISTANT CHIEF OF STAFF FOR
AUTOMATION & COMMUNICATIONS
ATTN DAMO-C4T
ATTN DAMO-C4S
DEPARTMENT OF THE ARMY
WASHINGTON, DC 20360

US ARMY BALLISTIC RESEARCH
LABORATORY
ATTN DRDAR-TSB-S (STINFO)
ABERDEEN PROVING GROUND, MD 21005

COMMANDER
US ARMY INFORMATION SYSTEMS COMMAND
ATTN CC-OPS-WR, O.P. CONNELL/R. NELSON
FT HUACHUCA, AZ 85613

COMMANDER
US ARMY ELECT SYS ENG
ATTN ASC-E-TS
FT HUACHUCA, AZ 85613

CHIEF
US ARMY INFORMATION SYSTEMS
MANAGEMENT AGENCY
DEPARTMENT OF THE ARMY
ATTN TECHNICAL DIRECTOR
FT MONMOUTH, NJ 07703

US ARMY COMBAT SURVEILLANCE & TARGET
ACQUISITION LABORATORY
ATTN DELET-DD
FT MONMOUTH, NJ 07703

US ARMY ENGINEER DIV HUNTSVILLE
DIVISION ENGINEER
ATTN HNDED FD, T. BOLT
PO BOX 1600
HUNTSVILLE, AL 35807

COMMANDER
US ARMY MATERIEL COMMAND
ATTN AMCRE
ATTN AMCDE
5001 EISENHOWER AVE
ALEXANDRIA, VA 22333-0001

DIRECTOR
US ARMY MATERIEL SYSTEMS ANALYSIS
ACTIVITY
ATTN DRXSY-MP, LIBRARY
ABERDEEN PROVING GROUND, MD 21005

COMMANDER
US ARMY MISSILE & MUNITIONS
CENTER & SCHOOL
ATTN ATSK-CTD-F
REDSTONE ARSENAL, AL 35809

COMMANDER
US ARMY NUCLEAR & CHEMICAL AGENCY
ATTN MONA-WE
7500 BACKLICK ROAD
SPRINGFIELD, VA 22150

DEP CH OF STAFF FOR RSCH, DEV, & ACQ
DEPARTMENT OF THE ARMY
ATTN DAMA-CSS-N
WASHINGTON, DC 20310

CHIEF
US ARMY SATELLITE COMMUNICATIONS
AGENCY
ATTN DRCPM-SC
FT MONMOUTH, NJ 07703

DIRECTOR
TRI/TAC
ATTN TT-E-SS, CHARNICK
FT MONMOUTH, NJ 07703

COMMANDER
NAVAL ELECTRONIC SYSTEMS COMMAND
ATTN PME 110-241D, D. O'BRYHIM, A. LARSON
WASHINGTON, DC 20360

CHIEF OF NAVAL MATERIEL
THEATER NUCLEAR WARFARE PROJECT OFFICE
ATTN PM-23, TN-31, TATE
WASHINGTON, DC 20360

COMMANDER
NAVAL OCEAN SYSTEMS CENTER
ATTN CODE 83, J. STAWISKI
SAN DIEGO, CA 92152

COMMANDING OFFICER
NAVAL ORDNANCE STATION
ATTN STANDARDIZATION DIVISION
INDIAN HEAD, MD 20640

COMMANDING OFFICER
NAVAL RESEARCH LABORATORY
ATTN CODE 4720, J. DAVIS
WASHINGTON, DC 20375

COMMANDER
NAVAL SURFACE WEAPONS CENTER
ATTN CODE F-56
DAHLGREN, VA 22448

COMMANDER
NAVAL SURFACE WEAPONS CENTER
ATTN CODE F32, E. RATHBURN
ATTN CODE F 30
WHITE OAK LABORATORY
SILVER SPRING, MD 20910

DEPARTMENT OF THE NAVY
DIRECTOR, NAVAL TELECOMMUNICATIONS
DIVISION
OFFICE OF THE CHIEF OF NAVAL OPERATIONS
ATTN OP941, HAISLMAIER
ATTN OP943
WASHINGTON, DC 20350

HQ, USAF/SAMI
WASHINGTON, DC 20330

AIR FORCE COMMUNICATIONS COMMAND
ATTN EPPD
SCOTT AFB, IL 62225

COMMANDER
US AIR FORCE SPACE COMMAND
ATTN KKO
ATTN KRQ
ATTN XPOW
PETERSON AFB, CO 80912

1842 EEC
ATTN EEISG
SCOTT AFB, IL 62225

HEADQUARTERS
ELECTRONIC SYSTEMS DIVISION/YS
ATTN YSEA
HANSCOM AFB, MA 01730

HEADQUARTERS
USAFE
ATTN DCKI
RAMSTEIN AFB, GERMANY

SYSTEM INTEGRATION OFFICE
ATTN SYE
PETERSON AFB, CO 80912

AIR FORCE WEAPONS LABORATORY/DYC
ATTN NTC4, TESD, IESM
KIRTLAND AFB, NM 87117

DIRECTOR
FEDERAL EMERGENCY MANAGEMENT AGENCY
NATIONAL PREPAREDNESS PROGRAM SUPPORT
ATTN OFFICE OF RESEARCH
WASHINGTON, DC 20472

DIRECTOR
FEDERAL EMERGENCY MANAGEMENT AGENCY
STATE & LOCAL SUPPORT BR
ATTN SL/EM/SS/LS, LOGISTICS
SUPPORT BRANCH
WASHINGTON, DC 20472

LAWRENCE LIVERMORE NATIONAL LAB
PO BOX 808
ATTN TECHNICAL INFO DEPT LIBRARY
ATTN L-156, H. CABAYAN, L. MARTIN
LIVERMORE, CA 94550

DIRECTOR
NATIONAL SECURITY AGENCY
ATTN R15
9800 SAVAGE ROAD
FT MEADE, MD 20755

AMERICAN TELEPHONE & TELEGRAPH CO
ATTN SEC OFC FOR W. EDWARDS
1120 20TH STREET, NW
WASHINGTON, DC 20036

AT&T BELL LABORATORIES
ATTN R. STEVENSON
ATTN J. MAY
1600 OSGOOD ST
N. ANDOVER, MA 01845

AT&T BELL LABORATORIES
ATTN J. SCHOOL
ATTN J. SERRI
CRAWFORDS CORNER ROAD
HOLMDEL, NJ 07733

BDM CORP
ATTN CORPORATE LIBRARY
7915 JONES BRANCH DRIVE
McLEAN, VA 22102

BDM CORP
ATTN L. O. HOEFT
1801 RANDOLPH RD, SE
ALBUQUERQUE, NM 87106

BOEING CC
PO BOX 3707
ATTN R. SHEPPE
SEATTLE, WA 98124

COMPUTER SCIENCES CORPORATION
SYSTEMS DIVISION
ATTN A. SCHIFF
1400 SAN MATEO BOVD, SE
ALBUQUERQUE, NM 87108

ELECTROMAGNETIC APPLICATIONS, INC
ATTN D. MEREWETHER
PO BOX 8482
ALBUQUERQUE, NM 87198

ELECTROMAGNETIC APPLICATIONS, INC
PO BOX 26263
ATTN R. PERALA
12567 W. CEDAR DR
LAKEWOOD, CO 80228-2091

ENSCO, INC
ATTN R. GRAY
540 PORT ROYAL RD
SPRINGFIELD, VA 22151

ENGINEERING SOCIETIES LIBRARY
ATTN ACQUISITIONS DEPT
345 E. 47TH ST
NEW YORK NY 10017

GEORGIA INSTITUTE OF TECHNOLOGY
OFFICE OF CONTRACT ADMINISTRATION
ATTN RES & SEC COORD FOR H. DENNY
ATLANTA, GA 30332

IIT RESEARCH INSTITUTE
ATTN J. BRIDGES
ATTN I. MINDEL
10 W 35TH STREET
CHICAGO, IL 60616

INTERNATIONAL TEL & TELEGRAPH CORP
ATTN A. RICHARDSON
ATTN TECHNICAL LIBRARY
500 WASHINGTON AVENUE
NUTLEY, NJ 07110

DISTRIBUTION (Cont'd)

KAMAN SCIENCES CORP
ATTN P. MADEL
SOUTH BAY CENTRE, SUITE 410
1515 W. 190TH ST
GARDENA, CA 90248

MISSION RESEARCH CORP
PO BOX 7816
ATTN W. STARKE
COLORADO SPRINGS, CO 80933

MISSION RESEARCH CORP
EM SYSTEM APPLICATIONS DIVISION
ATTN A. CHODOROW
1720 RANDOLF ROAD, SE
ALBUQUERQUE, NM 87106

R&D ASSOCIATES
PO BOX 9695
ATTN W. GRAHAM
ATTN TECHNICAL LIBRARY
MARINA DEL REY, CA 90291

SCIENCE APPLICATIONS, INC
PO BOX 1303
ATTN W. CHADSEY
MCLEAN, VA 22102

SRI INTERNATIONAL
ATTN G. AUGUST
ATTN A. WHITSON
ATTN E. VANCE
333 RAVENSWOOD AVENUE
MENLO PARK, CA 94025

TRW DEFENSE & SPACE SYSTEMS GROUP
ATTN J. PENAR
ONE SPACE PARK
REDONDO BEACH, CA 92078

TRW DEFENSE & SPACE SYSTEMS GROUP
ATTN E. P. CHIVINGTON
2240 ALAMO, SE
SUITE 200
ALBUQUERQUE, NM 87106

TRW, INC
COMMAND & CONTROL & COMMUNICATIONS
SYSTEM DIV
ATTN N. STAMMER
5203 LEESBURG PIKE
SUITE 310
FALLS CHURCH, VA 22041

US ARMY LABORATORY COMMAND
ATTN COMMANDER, AMSLC-CG
ATTN TECHNICAL DIRECTOR, AMSLC-TD
ATTN E. WELCH, AMSLC-TP-AS

INSTALLATION SUPPORT ACTIVITY
ATTN DIRECTOR, SLCIS-D
ATTN RECORD COPY, SLCIS-IM-TS
ATTN LIBRARY, SLCIS-IM-TL (3 COPIES)
ATTN LIBRARY, SLCIS-IM-TL (WOODBRIDGE)
ATTN TECHNICAL REPORTS BRANCH, SLCIS-IM-TR
ATTN LEGAL OFFICE, SLCIS-CC

HARRY DIAMOND LABORATORIES
ATTN D/DIVISION DIRECTORS
ATTN DIVISION DIRECTOR, SLCHD-RT
ATTN LAB DIRECTOR, SLCHD-NW-E
ATTN CHIEF, SLCHD-NW-EB
ATTN CHIEF, SLCHD-NW-EC
ATTN CHIEF, SLCHD-NW-ED (10 COPIES)
ATTN CHIEF, SLCHD-NW-EE (2 COPIES)
ATTN CHIEF, SLCHD-NW-P
ATTN CHIEF, SLCHD-NW-R
ATTN CHIEF, SLCHD-NW-RA
ATTN CHIEF, SLCHD-NW-RC
ATTN CHIEF, SLCHD-NW-RH
ATTN CHIEF, SLCHD-NW-RI
ATTN CHIEF, SLCHD-TT
ATTN B. ZABLUDOWSKI, SLCHD-IT-E
ATTN H. CORNWELL, SLCHD-IT-RT
ATTN L. AMBROSE, SLCHD-NW-EC
ATTN R. CHASE, SLCHD-NW-EC
ATTN W. COBURN, SLCHD-NW-EC
ATTN T. MAK, SLCHD-NW-EC
ATTN J. SWETON, SLCHD-NW-EC
ATTN H. ROBERTS, SLCHD-NW-RA (30 COPIES)